Hindawi
Shock and Vibration
Volume 2019, Article ID 7295615, 7 pages
https://doi.org/10.1155/2019/7295615

Research Article

A Simplified Finite Element Approach for Modeling of Multilayer Plates

Taiyou Liu,[1] Xinbo Ma,[1] Pak Kin Wong,[1] Jing Zhao,[1] Zhengchao Xie,[2] and V. A. Melo Cristino[1]

[1]*Department of Electromechanical Engineering, University of Macau, Taipa, Macau*
[2]*School of Mechanical and Automotive Engineering, South China University of Technology, Guangzhou, China*

Correspondence should be addressed to Jing Zhao; zhaojing003@163.com and Zhengchao Xie; zxie@scut.edu.cn

Received 2 August 2018; Accepted 31 December 2018; Published 10 February 2019

Academic Editor: Konstantin Avramov

The multilayer plate has a great potential for automotive and aerospace applications. However, the complexity in structure and calculation of the response impede the practical applications of multilayer plates. To solve this problem, this work proposes a new plate finite element and a simplified finite element (FE) model for multilayer plates. The proposed new plate finite element consists of the shear and extension strains in all layers. The multilayer structure with the proposed new plate finite element is regarded as a reference to calculate the reference value of the transverse response. The simplified FE model of multilayer plates is proposed based on the equivalent bending stiffness by curve fitting of the reference value of the transverse response. Numerical study shows that this approach can be used to set up the simplified FE model of multilayer plates.

1. Introduction

In recent decades, the multilayer plates have been demonstrated to be promising engineering structures for automobiles and aerospace vehicles [1–4]. A typical multilayer plate has three layers, including the constraint layer, damping layer, and base layer. The multilayer plate structure is mainly used for vibration suppression with the consumption of the strain energy since the damping layer would deform with the relative motion of the constraint layer and base layer [5–8]. Therefore, the strain in all layers should be well considered when modeling the multilayer plates.

In the literatures, extensive investigations have been conducted on the modeling of the multilayer plates [4, 6, 9–11]. However, an assumption is usually made that only shear train exists in the core layer and extension strain exists in the constraint layer and base layer [12]. This assumption is not valid for certain structures and conditions. Moreover, majority of researchers have studied the multilayer plate structure by presenting the analytical solutions using the modal superposition method. However, the analytical solution is quite complex and not accurate [13–15]. On the other hand, the finite element (FE) modeling is a good numerical method which has been extensively and efficiently applied to investigate the vibrational behavior of structures including the viscoelastic material [13, 14, 16–18]. However, when modeling this plate structure using the FE method, the plate is meshed into many finite elements and the degrees of freedom should be well defined with full consideration of the shear, compression, and extensional damping. For the complex modeling problem, the beam finite element presented by Zapfe and Lesieutre with 11 degrees of freedom (DOFs) can be referred with a very good FE model [19]. Moreover, the plate structure is an extension of beam structure. Considering the efficiency of FE method and accuracy of the structure of plates, the work tries to develop a new plate finite element consisting of the shear and extension strains in all layers as an extension of Zapfe's beam element.

Even though the plate structure with new plate finite element method can develop a good FE model, there are still plenty of DOFs involved, which makes the FE modeling of multilayer plate structures complicated, especially for the plate structure with a quite thin damping layer. To ease the computational burden and consumption cost, a simplified method should be developed. In [20], a simplified FE model for beam structures with three layers is presented by using single-layer equivalent FE method. The equivalent material properties are calculated and then a regular beam is constructed. Considering the simplicity and accuracy, this work also attempts to develop a simplified FE model for multilayer plates by curve fitting the equivalent bending stiffness.

In this research, a new plate finite element for multilayer plate is developed, and a simplified FE model of multilayer plates is proposed based on the equivalent bending stiffness by curve fitting the response values calculated from the multilayer plate structure with new plate finite element. The rest of this paper is organized as follows. Section 2 presents the proposed new plate finite element as an extension of Zapfe's beam element with validation. Subsequently, the simplified FE model for multilayer plates is described in Section 3. Finally, conclusions are given in Section 4.

2. New Plate Finite Element for Multilayer Plate

This section presents a new plate finite element for multilayer plate for FE modeling. First, the new plate finite element is proposed with the analysis of degree of freedom (DOF), and then a validation is conducted by comparison with the published data.

2.1. Proposed New Plate Finite Element for Multilayer Plate. The element formulated in the work of Zapfe and Lesieutre was used as the reference in the curve fitting of a transfer function of the multilayer beam [19]. This element can be extended to constrained layer damped plates. The basic formulations in the work of Zapfe and Lesieutre can be followed to develop the new plate elements with more degrees of freedom [19]. Figure 1 gives the multilayer plate studied in this work. It consists of three layers. Layer 1, layer 2, and layer 3 are the base layer, damping layer, and constraining layer, respectively. Figure 2 shows the DOFs of the new plate element. Each of the four nodes in every corner has eight longitudinal degrees of freedom and one transverse degree of freedom. Note that there are five additional midnodes in the element in order to avoid shear locking. These five midnodes have only one transverse degree of freedom.

As described in Figure 1, the DOF vector of each node can be given in the following equations. For nodes m, k, p, and q, there are four DOFs in the u and v directions, respectively, and one DOF in the w direction. For nodes 1, 2, 3, 4, and 5, only one DOF exists in the w direction. To fully characterize the shear strain and extension strain and clearly represent the transverse displacement at each location of the plate, the DOF vectors $\mathbf{U}_j\,(j = m, k, p, k, 1,\ 2,\ 3,\ 4,\ 5)$ are represented as

Figure 1: Multilayer plate.

$$\begin{aligned}
\mathbf{U}_m &= \left[u_{m1}, u_{m2}, u_{m3}, u_{m4}, v_{m1}, v_{m2}, v_{m3}, v_{m4}, w_m\right],\\
\mathbf{U}_k &= \left[u_{k1}, u_{k2}, u_{k3}, u_{k4}, v_{k1}, v_{k2}, v_{k3}, v_{k4}, w_k\right],\\
\mathbf{U}_p &= \left[u_{p1}, u_{p2}, u_{p3}, u_{p4}, v_{p1}, v_{p2}, v_{p3}, v_{p4}, w_p\right],\\
\mathbf{U}_q &= \left[u_{q1}, u_{q2}, u_{q3}, u_{q4}, v_{q1}, v_{q2}, v_{q3}, v_{q4}, w_q\right],\\
\mathbf{U}_1 &= w_1,\\
\mathbf{U}_2 &= w_2,\\
\mathbf{U}_3 &= w_3,\\
\mathbf{U}_4 &= w_4,\\
\mathbf{U}_5 &= w_5.
\end{aligned} \tag{1}$$

By combining all of the DOFs of each node, the DOF vector of the proposed new finite element for the multilayer plate can be expressed in the following equations:

$$\begin{aligned}
\mathbf{U} &= \left[\mathbf{U}_m, \mathbf{U}_1, \mathbf{U}_k, \mathbf{U}_2, \mathbf{U}_3, \mathbf{U}_4, \mathbf{U}_p, \mathbf{U}_5, \mathbf{U}_q\right]\\
&= [u_{m1}, u_{m2}, u_{m3}, u_{m4}, v_{m1}, v_{m2}, v_{m3}, v_{m4}, w_m, w_1, u_{k1}, u_{k2},\\
&\quad \cdot u_{k3}, u_{k4}, v_{k1}, v_{k2}, v_{k3}, v_{k4}, w_k, w_2, w_3, w_4, u_{p1}, u_{p2}, u_{p3},\\
&\quad \cdot u_{p4}, v_{p1}, v_{p2}, v_{p3}, v_{p4}, w_p, w_5, u_{q1}, u_{q2}, u_{q3}, u_{q4}, v_{q1}, v_{q2},\\
&\quad \cdot v_{q3}, v_{q4}, w_q].
\end{aligned} \tag{2}$$

It can be found that each finite element for the multilayer plate has 41 DOFs. During the FE modeling, the multilayer is meshed into many elements with n_x and n_y nodes in the longitudinal directions. The overall DOF in the multilayer plate structure can be expressed as

$$n_{\mathrm{DOF}} = 9n_x n_y + \left(3n_x - 2\right)\left(n_y - 1\right) + n_x - 1. \tag{3}$$

For each meshed element, a shape function matrix $\mathbf{N}\,(\mathbf{N} \in R^{3\times 12})$ for each layer can be defined as

$$\mathbf{N} = \begin{bmatrix} \mathbf{P}_1 \\ \mathbf{P}_2 \\ \mathbf{P}_3 \end{bmatrix} = \begin{bmatrix} n_1 & 0 & 0 & n_2 & 0 & 0 & n_3 & 0 & 0 & n_4 & 0 & 0 \\ 0 & n_1 & 0 & 0 & n_2 & 0 & 0 & n_3 & 0 & 0 & n_4 & 0 \\ 0 & 0 & n_1 & 0 & 0 & n_2 & 0 & 0 & n_3 & 0 & 0 & n_4 \end{bmatrix}, \tag{4}$$

where the shape function in matrix $\mathbf{N}$ can be written as $n_1 = y/l_y - xy/l_x l_y$, $n_2 = xy/l_x l_y$, $n_3 = 1 - x/l_x - y/l_y + xy/l_x l_y$, and $n_4 = x/l_x - xy/l_x l_y$. The variables x and y are the longitudinal coordinates; l_x and l_y are the length and width of each meshed element, respectively. By calculating the differences of matrices $\mathbf{P}_1$, $\mathbf{P}_2$, and $\mathbf{P}_3$, a new shape function $\mathbf{B}\,(\mathbf{B} \in R^{5\times 12})$ can be obtained:

$$\mathbf{B} = \left[\frac{\partial \mathbf{P}_1}{\partial x}; \frac{\partial \mathbf{P}_2}{\partial y}; \frac{\partial \mathbf{P}_1}{\partial y} + \frac{\partial \mathbf{P}_2}{\partial x}; \frac{\partial \mathbf{P}_3}{\partial x}; \frac{\partial \mathbf{P}_3}{\partial x}\right]. \tag{5}$$

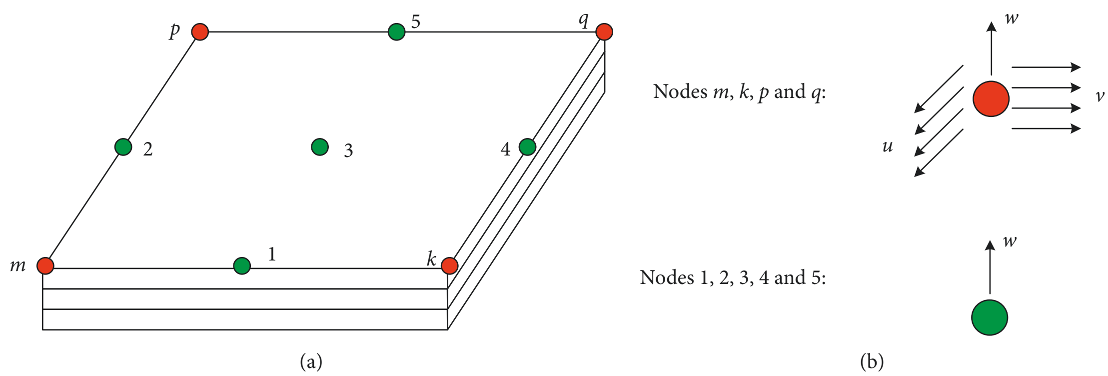

FIGURE 2: Analysis of DOF for the proposed new plate finite element for multilayer plate. (a) Proposed new plate finite element for multilayer plate. (b) Analysis of DOF for each node for multilayer plate.

Meanwhile, a modulus matrix $\mathbf{E}_c$ ($\mathbf{E}_c \in R^{5\times 5}$) with Young's modulus E and shear modulus G can be formulated as

$$\mathbf{E}_c = \begin{bmatrix} E & 0 & 0 & 0 & 0 \\ 0 & E & 0 & 0 & 0 \\ 0 & 0 & E & 0 & 0 \\ 0 & 0 & 0 & G & 0 \\ 0 & 0 & 0 & 0 & G \end{bmatrix}. \quad (6)$$

Then, the corresponding stiffness matrix **KK** and mass matrix **MM** of each meshed element in each layer can be set as

$$\mathbf{MM} = \rho \mathbf{P}^{\mathrm{T}} \mathbf{P}, \qquad \mathbf{KK} = \mathbf{B}^{\mathrm{T}} \mathbf{E}_c \mathbf{B}, \quad (7)$$

where ρ is the density of the plate. Since the multilayer plate is meshed in many plate finite elements, the stiffness matrix **K** and mass matrix **M** can be obtained by integrating the stiffness matrix **KK** and mass matrix **MM** of each plate finite element in the plate structure. By exciting a given force vector, the response can be obtained according to the Lagrange formula [21]:

$$\mathbf{M}\ddot{\mathbf{X}} + \mathbf{K}\mathbf{X} = \mathbf{F}, \qquad \mathbf{X} = \mathbf{F}\left[\mathbf{K} - \omega^2 \mathbf{M}\right]^{-1}, \quad (8)$$

where **F** stands for the excited force vector; ω represents the inherent frequency of the multilayer plate structure; and **X** is the response matrix of the multilayer plate with meshed plate finite elements. The response matrix **X** can be obtained by combining the matrix **U** in each plate finite element.

2.2. Validation of Proposed New Plate Finite Element. After the plate element is formulated, it should be validated to illustrate its effectiveness. In the existing literature, Kung and Singh provided some results calculated by the analytical model developed for the beam element in their work [22]. Naturally, these data can be used here to validate the plate element. Table 1 gives the configuration of a plate to be validated which is simply supported along all four edges.

TABLE 1: Plate parameters for validation.

Properties	Layer 1	Layer 2	Layer 3
Density (kg/m^3)	7800	2000	7800
Young's modulus (Pa)	207e9	12e6	207e9
Shear modulus (Pa)	80e9	4e6	80e9
Thickness (m)	0.002	0.002	0.002
Length (m)	0.4	0.4	0.4
Width (m)	0.4	0.4	0.4
Loss factor	0	0.38	0

The comparison of the frequency and loss factor between the published data [22] and the data calculated by the new plate element is presented in Tables 2 and 3, respectively. From Tables 2 and 3, it can be seen that the new plate element provides close results to the published data in the work of Kung and Singh by predicting the natural frequencies and loss factors. The difference of frequency between the data in Kung and Singh and new plate finite element at each mode is less than 9%, while the difference of loss factor is less than 16%. The biggest differences of frequency and loss factor are 8.8% and 15.9%, respectively. The biggest difference appears at the mode (1, 1) with the lowest frequency and highest loss factor. Moreover, both the differences of frequency and loss factor decrease along with the increase of the mode. Thus, the proposed new finite element matches well with the published data, especially for high modes. As a result, the multilayer with the proposed new finite element can be used as the reference to regress the equivalent plate bending stiffness as described.

3. Simplified FE Model for Multilayer Plates

This section presents the simplified FE model for multilayer plates. First, the equivalent bending stiffness is derived by using curve fitting method. Then, a simplified FE model is developed and simulated by applying the equivalent bending stiffness to a regular single-layer plate element.

3.1. Identification of Equivalent Bending Stiffness. Since there is no closed-form solution for the multilayer plate structure, an example is given here based on the curve fitting of the

Table 2: Comparison of frequency between the data in Kung and Singh [22] and new plate finite element.

Mode	Results of Kung and Singh [22]	New element	Difference (%)
(1, 1)	975 Hz	889 Hz	8.8
(1, 2)	2350 Hz	2207 Hz	6.1
(2, 1)	2350 Hz	2207 Hz	6.1
(2, 2)	3725 Hz	3511 Hz	5.7

Table 3: Comparison of loss factor between the data in Kung and Singh [22] and new plate finite element.

Mode	Results of Kung and Singh [22]	New element	Difference (%)
(1, 1)	0.044	0.051	15.9
(1, 2)	0.019	0.021	10.5
(2, 1)	0.019	0.021	10.5
(2, 2)	0.012	0.013	8.3

response, instead of the transfer function, in order to derive the equivalent plate bending stiffness. At first, the transverse vibration response can be calculated analytically by using a modal superposition method [23]. Then, this response can be regressed according to the reference value calculated by the proposed new plate element in Section 2. For a clamped multilayer plate considered here, Table 4 gives the parameters. A unit amplitude harmonic force is applied on the center of the multilayer plate, as shown in Figure 3. Figure 4 shows the response at the center of the multilayer plate under different frequencies. This response is used as the reference to regress the response calculated by the analytical modal superposition method. In this work, an undamped multilayer plate is used in the numerical example of regression of the equivalent bending stiffness of the plate structure.

The approach for obtaining equivalent properties is described in the following. The analytically calculated response is regressed based on the reference value at the first two resonances. Subsequently, with equation (8), the equivalent bending stiffness can be calculated with corresponding stiffness matrix. In this example, the resonances are selected at the frequencies of around 75 Hz and 285 Hz. Then, a line/curve can be obtained by fitting the two obtained equivalent bending stiffness at the two resonant frequencies. Figure 5 demonstrates how a smooth curve fits to the two resonant frequencies in order to determine bending stiffness. It should be noted that this example just shows the basic idea of extracting equivalent properties. In reality, the curve fitting should be conducted for more resonant frequencies.

3.2. Development and Simulation of Simplified FE Model. After the equivalent multilayer plate bending stiffness is derived, it is applied to the regular single-layer plate structure to set up the simplified FE model. For the single-layer plate structure, the same nodes are used to present the DOF as the multilayer plate structure, as shown in Figure 6. By combining all of the DOFs of each node, the DOF vector of the proposed new finite element for single-layer plate can be expressed in the following equations:

Table 4: Plate parameters for curve fitting.

Properties	Layer 1	Layer 2	Layer 3
Density (kg/m^3)	7800	2000	7800
Young's modulus (Pa)	2e11	2e6	2e11
Shear modulus (Pa)	8e10	8e5	8e10
Thickness (m)	0.001	0.001	0.001
Length (m)	0.4	0.4	0.4
Width (m)	0.4	0.4	0.4
Loss factor	0	0	0

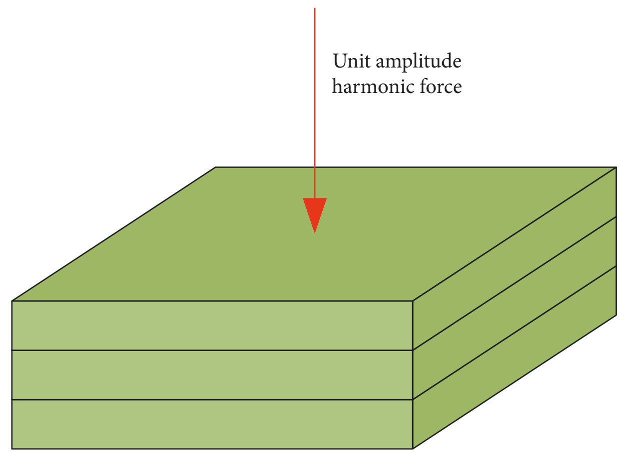

Figure 3: Unit amplitude harmonic force applied on the center of the multilayer plate.

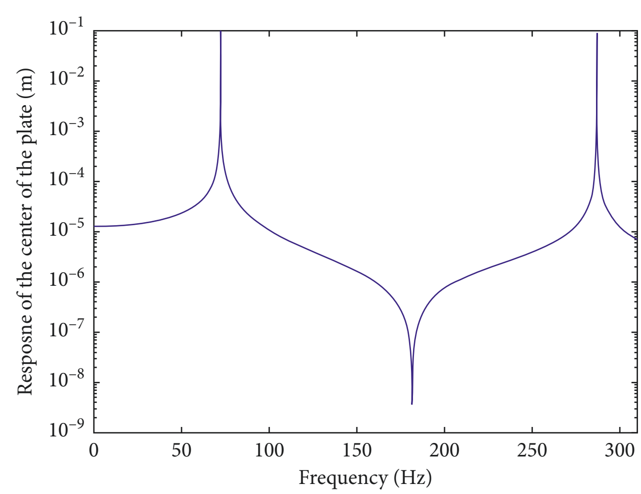

Figure 4: Response of the center of the multilayer plate calculated with the new plate element.

$$\begin{aligned}\mathbf{U}_s &= \left[\mathbf{U}_{ms}, \mathbf{U}_{1s}, \mathbf{U}_{ks}, \mathbf{U}_{2s}, \mathbf{U}_{3s}, \mathbf{U}_{4s}, \mathbf{U}_{ps}, \mathbf{U}_{5s}, \mathbf{U}_{qs}\right] \\ &= \left[u_{ms1}, u_{m2}, v_{ms1}, v_{ms2}, w_{ms}, w_{s1}, u_{sk1}, u_{sk2}, v_{ks1}, v_{ks2}, w_{sk},\right. \\ &\quad \cdot w_{s2}, w_{s3}, w_{s4}, u_{ps1}, u_{ps2}, v_{ps1}, v_{ps2}, w_{ps}, w_{s5}, u_{qs1}, u_{qs2}, \\ &\quad \left.\cdot v_{qs1}, v_{qs2}, w_{qs}\right].\end{aligned} \tag{9}$$

Based on the defined DOF vectors, it can be seen that each finite element for the single-layer plate has 25 DOFs. For the meshed multilayer plate structure, the overall DOF is

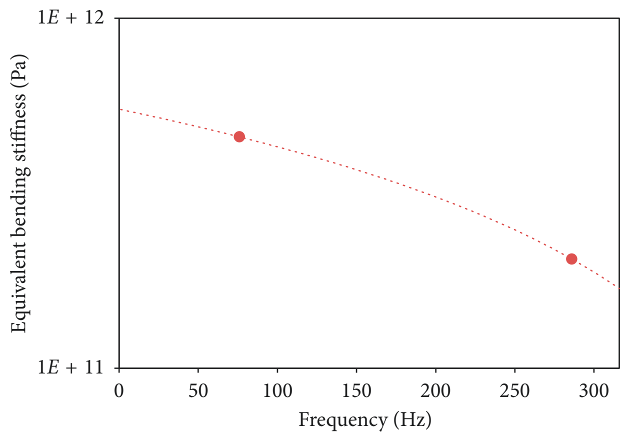

FIGURE 5: Equivalent bending stiffness obtained for simplified FE model.

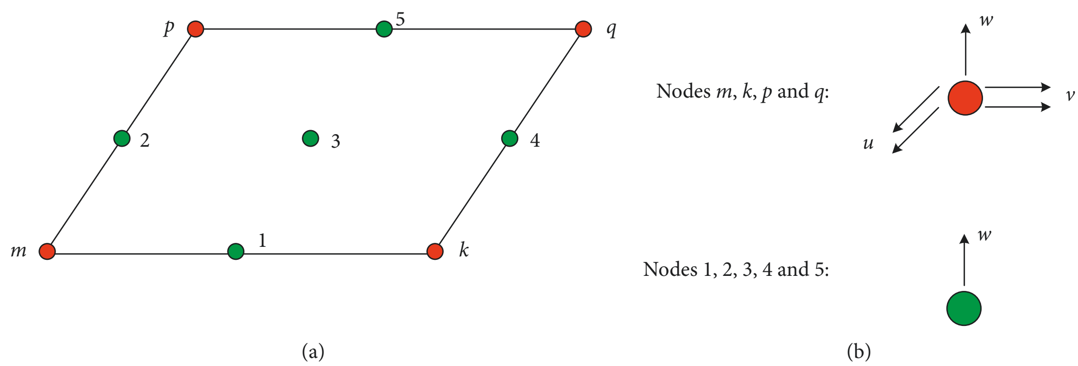

FIGURE 6: Analysis of DOF for the proposed new plate finite element for the single-layer plate. (a) Proposed new plate finite element for the single-layer plate. (b) Analysis of DOF for each node for the single-layer plate.

$$n_{\mathrm{sDOF}} = 5n_x n_y + (3n_x - 2)(n_y - 1) + n_x - 1. \quad (10)$$

After defining the DOF vector of the proposed new finite element for the single-layer plate, the corresponding stiffness matrix and mass matrix can be set based on the boundary conditions and equivalent multilayer bending stiffness. With the given stiffness matrix and mass matrix, the response of the regular single-layer plate structure can be obtained according to the Lagrange formula presented in equation (4).

3.3. Simulation of Simplified FE Model. Figure 7 shows the comparison between the reference and the response calculated with a simplified FE model. It can be seen that they match well in most frequency ranges except in the frequency range of antiresonance. The frequencies of resonances calculated by a simplified FE model are in good agreement with the reference. The difference of frequency at the antiresonance is less than 10%. Even though the frequency of antiresonance is a little different, the response values obtained by two methods are almost the same. The goal of this example is to show the possible solution of setting up the simplified FE model for multilayer plates. As a result, this approach can be used to effectively set up the simplified FE model of multilayer plates. Besides, the approach can be improved by curve fitting over more resonances or deriving approximate solutions of the plate transverse displacements in order to derive the transfer function. The latter can be

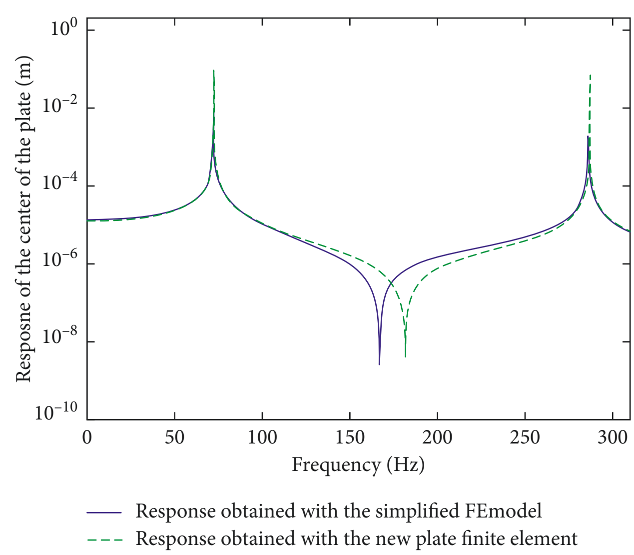

FIGURE 7: Comparison between the responses calculated with the simplified FE model and the reference value calculated with the new plate element.

better because the transfer function contains more structural characteristics than the simple response, so it will be considered as a future work.

4. Conclusions

This paper proposes a new plate finite element as an extension of Zapfe's beam element and a simplified FE model of multilayer plates. First, the new plate finite element is developed as a reference. Then, the curve fitting approach is applied to multilayer plates with the reference value to derive the equivalent bending stiffness. Finally, a simplified FE model of multilayer plates is proposed by applying the derived equivalent bending stiffness to a regular single-layer plate structure. The numerical example shows that this approach can be used to effectively set up the simplified FE model of multilayer plates.

In terms of applications, the proposed method can provide guidance in model development for the active vibration control of high-performance light weight smart structures, such as wind turbine, helicopter and aircraft structures, and so on. In addition, the approach can be further improved by curve fitting over more resonances or deriving approximate solutions in the future. Also, the plates with different boundary conditions and loading modes should be studied in future works. In addition, the simplified modeling of the multilayer plate with rotation will be further investigated.

Data Availability

The data used to support the findings of this study are included within the article.

Conflicts of Interest

The authors declare that they have no conflicts of interest.

Acknowledgments

This work was supported by the Science and Technology Development Fund of Macau S.A.R. under grant no. 012/2015/A, the Research Grant of the University of Macau under grant nos. MYRG2016-00212-FST and MYRG2017-00135-FST, and the National Natural Science Foundation of China under grant no. 51705084. This work was also supported by the Natural Science Foundation of Guangdong Province of China (grant no. 2018A030313999) and Fundamental Research Funds for the Central Universities (grant no. 2018MS46).

References

[1] H. Chan, B. Masserey, and P. Fromme, "High frequency guided ultrasonic waves for hidden fatigue crack growth monitoring in multi-layer model aerospace structures," *Smart Materials and Structures*, vol. 24, no. 2, pp. 25–37, 2015.

[2] L. Fan, Z. Chen, S.-y. Zhang, J. Ding, X.-j. Li, and H. Zhang, "An acoustic metamaterial composed of multi-layer membrane-coated perforated plates for low-frequency sound insulation," *Applied Physics Letters*, vol. 106, no. 15, pp. 457–131, 2015.

[3] M. Shariyat and M. Roshanfar, "A new analytical solution and novel energy formulations for non-linear eccentric impact analysis of composite multi-layer/sandwich plates resting on point supports," *Thin-Walled Structures*, vol. 127, pp. 157–168, 2018.

[4] Y. Zhou, Q. Wang, D. Shi, Q. Liang, and Z. Zhang, "Exact solutions for the free in-plane vibrations of rectangular plates with arbitrary boundary conditions," *International Journal of Mechanical Sciences*, vol. 130, pp. 1–10, 2017.

[5] W. Zheng, Y. Lei, S. Li, and Q. Huang, "Topology optimization of passive constrained layer damping with partial coverage on plate," *Shock and Vibration*, vol. 20, no. 2, pp. 199–211, 2013.

[6] Q. Wang, K. Choe, D. Shi, and K. Sin, "Vibration analysis of the coupled doubly-curved revolution shell structures by using Jacobi-Ritz method," *International Journal of Mechanical Sciences*, vol. 135, pp. 517–531, 2018.

[7] Q. Wang, D. Shao, and B. Qin, "A simple first-order shear deformation shell theory for vibration analysis of composite laminated open cylindrical shells with general boundary conditions," *Composite Structures*, vol. 184, pp. 211–232, 2018.

[8] Q. Wang, B. Qin, D. Shi, and Q. Liang, "A semi-analytical method for vibration analysis of functionally graded carbon nanotube reinforced composite doubly-curved panels and shells of revolution," *Composite Structures*, vol. 174, pp. 87–109, 2017.

[9] X. Guan, J. Tang, D. Shi, C. shuai, and Q. Wang, "A semi-analytical method for transverse vibration of sector-like thin plate with simply supported radial edges," *Applied Mathematical Modelling*, vol. 60, pp. 48–63, 2018.

[10] J. Zhao, P. K. Wong, X. Ma, Z. Xie, J. Xu, and V. A. Cristino, "Simplification of finite element modeling for plates structures with constrained layer damping by using single-layer equivalent material properties," *Composites Part B: Engineering*, vol. 157, pp. 283–288, 2019.

[11] J. Zhao, Q. Wang, X. Deng, K. Choe, F. Xie, and C. Shuai, "A modified series solution for free vibration analyses of moderately thick functionally graded porous (FGP) deep curved and straight beams," *Composites Part B: Engineering*, vol. 165, pp. 155–166, 2019.

[12] Z. Xie and X. Xue, "A new plate finite element model for rotating plate structures with constrained damping layer," *Finite Elements in Analysis and Design*, vol. 47, no. 5, pp. 487–495, 2011.

[13] X. Guan, J. Tang, Q. Wang, and C. shuai, "Application of the differential quadrature finite element method to free vibration of elastically restrained plate with irregular geometries," *Engineering Analysis with Boundary Elements*, vol. 90, pp. 1–16, 2018.

[14] P. K. Wong, Z. Xie, J. Zhao, T. Xu, and F. He, "Analysis of automotive rolling lobe air spring under alternative factors with finite element model," *Journal of Mechanical Science and Technology*, vol. 28, no. 12, pp. 5069–5081, 2014.

[15] J. Zhao, Q. Wang, X. Deng, K. Choe, R. Zhong, and C. Shuai, "Free vibrations of functionally graded porous rectangular plate with uniform elastic boundary conditions," *Composites Part B: Engineering*, vol. 168, pp. 106–120, 2019.

[16] A. Castel, A. Loredo, A. El Hafidi, and B. Martin, "Complex power distribution analysis in plates covered with passive constrained layer damping patches," *Journal of Sound and vibration*, vol. 331, no. 11, pp. 2485–2498, 2012.

[17] J. F. A. Madeira, A. L. Araújo, and C. M. Mota Soares, "Multiobjective optimization of constrained layer damping

treatments in composite plate structures," *Mechanics of Advanced Materials and Structures*, vol. 24, no. 5, pp. 427–436, 2016.

[18] K. Choe, J. Tang, C. Shui, A. Wang, and Q. Wang, "Free vibration analysis of coupled functionally graded (FG) doubly-curved revolution shell structures with general boundary conditions," *Composite Structures*, vol. 194, pp. 413–432, 2018.

[19] J. A. Zapfe and G. A. Lesieutre, "A discrete layer beam finite element for the dynamic analysis of composite sandwich beams with integral damping layers," *Computers & Structures*, vol. 70, no. 6, pp. 647–666, 1999.

[20] Z. Xie and W. Steve Shepard Jr., "Development of a single-layer finite element and a simplified finite element modeling approach for constrained layer damped structures," *Finite Elements in Analysis and Design*, vol. 45, no. 8-9, pp. 530–537, 2009.

[21] Z. Xie, W. Steve Shepard Jr., and K. A. Woodbury, "Design optimization for vibration reduction of viscoelastic damped structures using genetic algorithms," *Shock and Vibration*, vol. 16, no. 5, pp. 455–466, 2009.

[22] S.-W. Kung and R. Singh, "Vibration analysis of beams with multiple constrained layer damping patches," *Journal of Sound and Vibration*, vol. 212, no. 5, pp. 781–805, 1998.

[23] C.-C. Sung and J. T. Jan, "The response of and sound power radiated by a clamped rectangular plate," *Journal of Sound and Vibration*, vol. 207, no. 3, pp. 301–317, 1997.

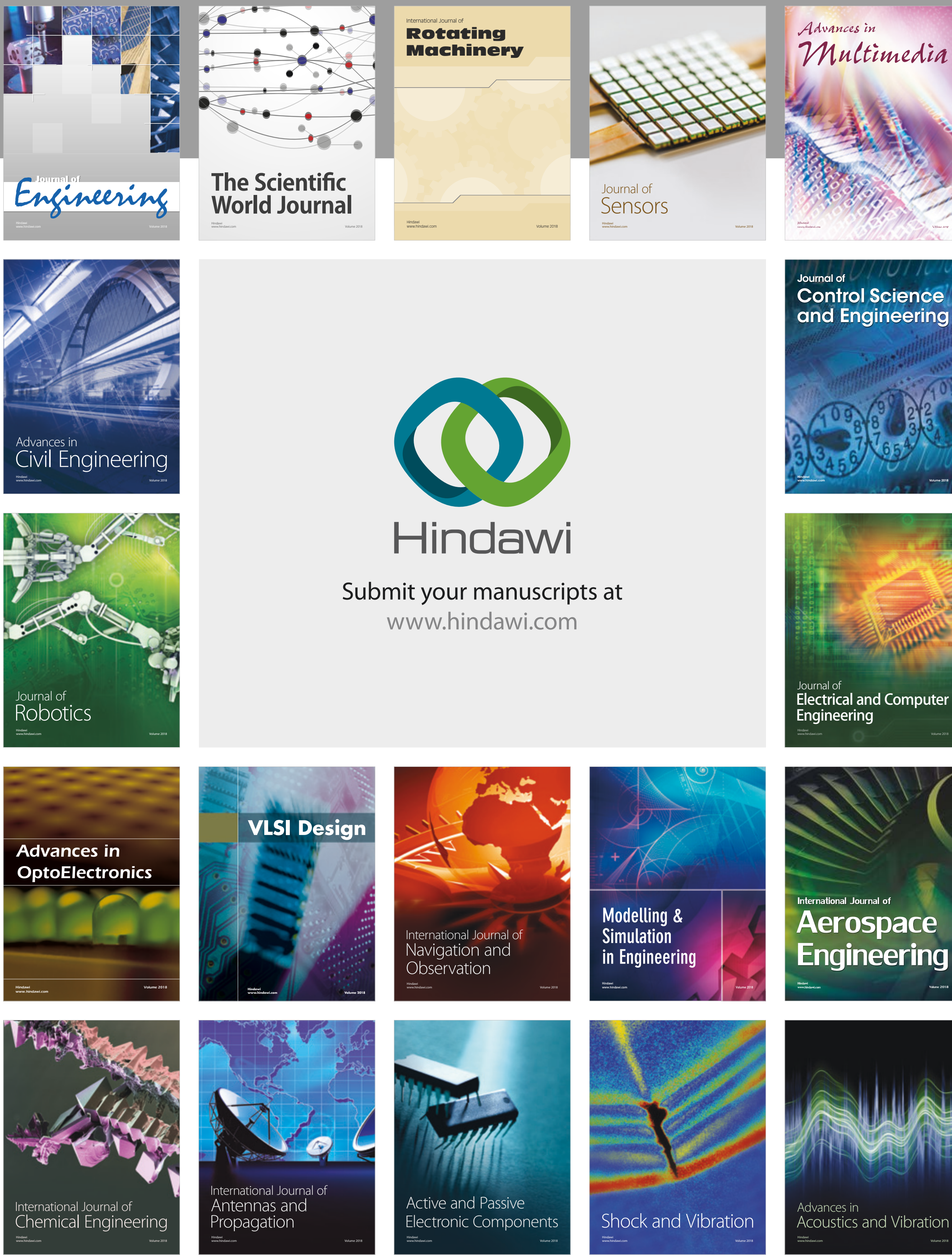

Journal of Engineering
The Scientific World Journal
International Journal of Rotating Machinery
Journal of Sensors
Advances in Multimedia
Advances in Civil Engineering
Hindawi
Submit your manuscripts at
www.hindawi.com
Journal of Control Science and Engineering
Journal of Robotics
Journal of Electrical and Computer Engineering
Advances in OptoElectronics
VLSI Design
International Journal of Navigation and Observation
Modelling & Simulation in Engineering
International Journal of Aerospace Engineering
International Journal of Chemical Engineering
International Journal of Antennas and Propagation
Active and Passive Electronic Components
Shock and Vibration
Advances in Acoustics and Vibration